The Effect of Helicopter Configuration on the Fluid Dynamics of Brownout

Catriona Phillips *
c.phillips@aero.gla.ac.uk

Richard E. Brown
rbrown@aero.gla.ac.uk

Department of Aerospace Engineering, University of Glasgow
Glasgow G12 8QQ, United Kingdom

Abstract

Brown's Vorticity Transport Model, coupled to an additional particle transport model, is used to simulate the development of the dust cloud that can form around a helicopter when operating in dusty or desert conditions. The flow field around a tandem rotor configuration is simulated during the final stages of landing. The time-averaged flow field around the helicopter is characterised by the existence of two stationary points immediately adjacent to the ground plane. Almost all entrainment of dust into the flow takes place forward of the rearmost stationary point; the dust initially remains in a thin, sheet-like layer above the ground. As the dust sheet approaches the forward stationary point, the layer thickens and forms a characteristic wedge-shaped 'separation zone'. The amount of sand that is subsequently drawn up away from the ground then appears to be critically dependent on the strength and position relative to the separation zone of strong regions of recirculation. VTM simulations suggest that, for a tandem rotor helicopter at least, the sudden growth of the dust cloud that is responsible for the onset of brownout may be due to a change in mode within the flow field surrounding the aircraft. At higher advance ratios the flow is dominated by a strong ground vortex that is created by the rear rotor. The forward extent of the resultant dust cloud is limited though by the absence of any strong recirculation within the flow below the front rotor of the system. At lower forward speed the ground vortex of the rear rotor is replaced by a strong vortex that lies just below the leading edge of the front rotor. This vortex is responsible for drawing a significant amount of dust out of the surface layer of entrained particulates to form a dense wall of dust some distance upstream of the helicopter. A study of the effect of blade twist on the strength and shape of the dust cloud formed in the flow surrounding helicopters with tandem rotors suggests that systems with smaller blade twist but the same disc loading might produce denser dust clouds than those with high blade twist.

Nomenclature

C_T	rotor thrust, scaled by $\rho A(\Omega R)^2$
d	particle diameter
g	acceleration due to gravity
R	rotor radius
S_ω	source of vorticity
S_p	source of particulates
t	time
μ	advance ratio
$\mu^\star$	thrust normalised advance ratio, $\mu/\sqrt{C_T/2}$
ν	fluid viscosity
ν_p	particle diffusion constant
ρ	air density
ρ_p	local density of particulates in air
ρ_s	material density of particles
υ	local flow velocity
υ_t	threshold velocity
υ_b	local on-blade velocity
υ_g	fallout velocity due to gravity
ω	vorticity
ω_b	blade bound vorticity

Introduction

The entrainment of dust into the air surrounding the rotorcraft when operating close to the ground is a particular concern to helicopter operators in desert conditions. Large clouds of dust can accumulate around the aircraft, and these can obscure the pilot's view particularly when taking off and landing. This can result in a loss of situational awareness and the potentially dangerous condition known as 'brownout.' Although an entirely aerodynamic solution to this problem is unlikely, a better understanding of the fluid dynamics of brownout might lead to ways of reducing its impact on desert operations.

To date there have been very few studies published which examine in detail the formation of brownout, and in particular the physics that governs its onset. There are, however, some reports from flight tests that show the distribution of dust within the air surrounding various aircraft in a variety of different flight conditions (Refs. 1 and 2). Although there is limited data avail-

*Presented at the 34th European Rotorcraft Forum, Liverpool, UK, September 16 - 19, 2008.

able on particle transport in the context of helicopter brownout, a large body of possibly relevant information has been built up in the field of riverine and aeolian sedimentology, and, indeed, several empirical models describing the behaviour of particles as they become suspended in water or air have been developed that may be applicable to the helicopter brownout problem.

Two approaches have been adopted previously to model the formation and evolution of brownout, one where individual particles are modelled and the other where the overall dynamics of the particle distribution are modelled. In the first, so-called Lagrangian approach, the trajectories of a large number of individual particles that represent the dust lifted from the ground plane are simulated to show the development of the dust cloud and the eventual onset of brownout. The dynamics of the particles introduced to the flow are modelled directly, for example using a Stokes-type drag law, as they are carried with the airflow generated by the helicopter (Ref. 3). Although good qualitative results can be achieved with this method a very large number of particles must be used if the variation of dust density within the flow is to be estimated reliably. The computational requirements of this approach can thus become very large. The second, so-called Eulerian approach is to model the overall dynamics of the particle distribution in the air surrounding the helicopter. Using this approach, the evolution of the dust cloud, described in terms of its local density, is calculated directly using suitable transport equations. The Eulerian approach has been used by Ryerson *et al.* (Ref. 4) and Haehnel *et al.* (Ref. 5) to model helicopter brownout. Both works claimed to use a two-phase flow model to represent the dynamics of the suspended particulate matter within the airflow, but it was assumed that there was only one-way coupling between the fluid and the suspended particulate matter. In other words, the effect of the fluid on the particles was considered but the effect of the particles on the flow was not.

In this paper, Brown's Vorticity Transport Model (Refs. 6 and 7) is used, together with an extension to the model which allows the entrainment of particles into the flow and their subsequent transport to be simulated, to model the onset and development of the brownout cloud that is induced by a helicopter operating in strong ground effect in dusty conditions. The Eulerian particle transport model that was used to produce the results presented in this paper is described in more detail by Phillips and Brown (Ref. 8). Their derivation of their particle transport model from a rigorous basis in the classical statistical mechanics of a distribution of particles adds to the existing body of work in the area by showing how the application of the Eulerian approach to the modelling of helicopter brownout can be rigorously justified subject to certain testable assumptions. The similarity between the resulting particle transport equation and the vorticity transport equation results in a particularly efficient computational model of the brownout problem within the framework of the VTM. The best approach to modelling the entrainment of particulates from the ground into the air in the context of helicopter brownout is still open to investigation, however. In the approach adopted here, a model for the physics of the entrainment process is constructed by adapting a sequence of empirical correlations that have been developed within the sedimentology community.

The resulting model is used to investigate how the initial entrainment of particles from the ground plane and the subsequent evolution of the particle density distribution relates to the velocity and vorticity within the flow field. The model is then used to simulate a generic tandem rotor helicopter operating in strong ground effect above a dusty surface. The effect of varying the blade twist on the geometry and extent of the dust cloud that is produced by this helicopter is then examined.

Vorticity and Particle Transport Models

Brown's Vorticity Transport Model (Refs. 6 and 7) has been adapted to include a model for the entrainment and transport of particulates in the airflow surrounding a helicopter in ground effect. The VTM is a finite volume method which uses a structured computational mesh to calculate the unsteady flow field around the aircraft by evolving the solution to the vorticity-velocity form of the unsteady, incompressible Navier-Stokes equation,

$$\frac{\partial}{\partial t}\omega + \upsilon \cdot \nabla\omega - \omega \cdot \nabla\upsilon = S_\omega + \nu\nabla^2\omega \qquad (1)$$

The differential form of the Biot-Savart relationship, $\nabla^2\upsilon = -\nabla \times \omega$, is used to relate the velocity, υ, to the vorticity, ω. The vorticity source, S_ω, arises in the shed and trailed vorticity from each lifting surface immersed within the flow and can be written as

$$S_\omega = -\frac{d}{dt}\omega_b + \upsilon_b \nabla \cdot \omega_b \qquad (2)$$

where ω_b is the bound vorticity associated with each lifting surface.

The particle transport model which governs the dynamics of a large number of suspended particles in the Eulerian frame of reference can be derived by adopting the formalism of classical statistical mechanics (Ref. 8). This transport equation can be written as

$$\begin{aligned}\frac{\partial}{\partial t}\rho_p \quad + \quad & (\upsilon + \upsilon_g) \cdot \nabla\rho_p = S_p + \nu_p\nabla^2\rho_p \\ & + \text{other non-equilibrium terms} \qquad (3)\end{aligned}$$

where the source term S_p allows particles to be introduced to the flow by entrainment from the ground plane. The velocity υ_g is the fallout velocity of the particulates due to the effect of gravity. The other terms on the right hand side of this equation can be included to model more accurately particle diffusion and other non-equilibrium processes such as spin-out from vortex cores.

The limitations on the applicability of Eq. 3 to the transport of particulates in the flow around the helicopter are derived in Ref. 8. Specifically it is shown that, if the non-equilibrium terms are ignored, then the ratio of particle drag to mass must be much greater than the accelerations within the flow field for the model to represent accurately the dynamics of the particulates in the flow. In most helicopter-related flows, this assumption holds well for the small particles of dust, clay and sand that are primarily responsible for brownout. For other applications where the dynamics of larger particles within the flow field might be important, some of the non-equilibrium terms in Eq. 3 may need to be retained, however.

The particulate source term, S_p, is implemented using a 'sublayer' type model that relates the flux of dust from the ground into the air to the motion of the particulates within the flow just above the ground. The physics of this entrainment process is very complex. It is thought that once a minimum threshold velocity is reached, the largest particles creep and saltate across the ground. The large particles then dislodge the smallest particles from the ground and these then become suspended within the airflow. Modelling the dynamics of the saltation and entrainment process directly would be very involved and is beyond the current state of the art. There are however a number of semi-empirical models available from within the sedimentology community that describe this process. Several of these can be adapted to model the flux of particulates from the ground into the air. In the present work, the theory of White (Ref. 9) has been used to determine the saltation or horizontal particle flux, Q. This flux is related to the flow velocity at the surface by

$$Q = Ec\upsilon^3 \frac{\rho}{g}\left(1-\frac{\upsilon_t}{\upsilon}\right)\left(1+\frac{\upsilon_t^2}{\upsilon^2}\right) \tag{4}$$

where, empirically, $c = 0.261$ and E is the ratio of erodible to total surface area taken here to be unity. The threshold velocity, υ_t, as described by Lu and Shao (Ref. 10) is related to the particle diameter and density by

$$\upsilon_t = \frac{1}{\kappa}\sqrt{a_1\left(\frac{\rho_s}{\rho}gd + \frac{a_2}{\rho d}\right)} \tag{5}$$

where κ accounts for the presence of surface roughness elements and the coefficients a_1 and a_2, based on wind tunnel experiments, are approximately 0.0123 and $3 \times 10^{-4}\mathrm{kgs}^{-2}$ respectively.

The relation between the saltation particle flux and the flux of particulates from the ground into the air, as described in Ref. 11, is

$$S_p = Q\, e^{13.4f-6.0} \tag{6}$$

where f is a measure of the clay content of the surface. S_p can then be interpreted as the source of particulates on the right hand side of the particle transport equation (Eq. 3).

There are obvious similarities in mathematical form between the vorticity transport equation (Eq. 1) and the the particle transport equation (Eq. 3). An additional stretching term appears in the vorticity transport equation simply to account for the fact that vorticity is vectorial in nature whereas the particulate density is scalar. The similarity between these two equations allows the particle transport equation to be evolved alongside the vorticity transport equation already implemented within the VTM without any significant increase in computational expense.

Verifiying the Predictions of Rotor Flows in Ground Effect

To obtain a reliable starting point for the modelling of brownout, the flow field around a helicopter in strong ground effect must first be shown to be modelled accurately. In this vein, Whitehouse and Brown (Ref. 12) and Phillips and Brown (Ref. 8) have shown, for instance, that the VTM is able to predict the existence of the various flow regimes, defined by Curtiss *et al.* (Ref. 13), that the rotor can experience when flown in ground effect at various different advance ratios. Further work has shown that the power required to hover in ground effect with a constant thrust as predicted by the VTM corresponds well with flight test data and the empirical correlations of Hayden (Ref. 14), Knight and Hefner (Ref. 15) and Cooke and Fitzpatrick (Ref. 16).

Verification of the ability of the VTM to predict rotor behaviour in ground effect has been continued by examining its ability to model the outwash in the wake of a hovering rotor. The flight test data of Harris and Simpson (Ref. 17) as documented by Preston (Ref. 18) has been used to compare the outwash velocity predicted by the VTM to that measured below a hovering CH-53E. Flight tests were carried out at three rotor heights with a range of different disc loadings, and outwash velocity profiles were measured at a number of radial distances from the rotor centre. A sample comparison between VTM predictions and the test data for the helicopter hovering at a rotor height of two radii above the ground (at a thrust coefficient of 0.0072) is presented in Fig. 1. The VTM data have been averaged over approximately 20 rotor revolutions after allowing the initial transients from the starting vortex to dissipate. There is significant unsteadiness in the flow below the rotor, even in hover, and the error bars attached to the numerical data represent the standard deviation of the predicted velocity over this time. The velocity profiles predicted using the VTM match the flight test data very well between the radial distances of $1.25R$ and $2R$. At the two innermost locations of $0.8R$ and $1.0R$ the comparison is not particularly good, however, with the flight test data, somewhat curiously, showing a strong jet wake to have already formed well underneath the rotor. The numerical results suggest that the jet forms somewhat further outboard. This discrepancy may be related to the absence of a fuselage in the calculations. The VTM also underpredicts the velocities at the furthest radial station from the rotor that was compared with the experimental data. This may be due to a slight excess of numerical dissipation within the calculations, or possibly to the calculations not having been run for long enough for the velocity profile this far from the rotor to have estab-

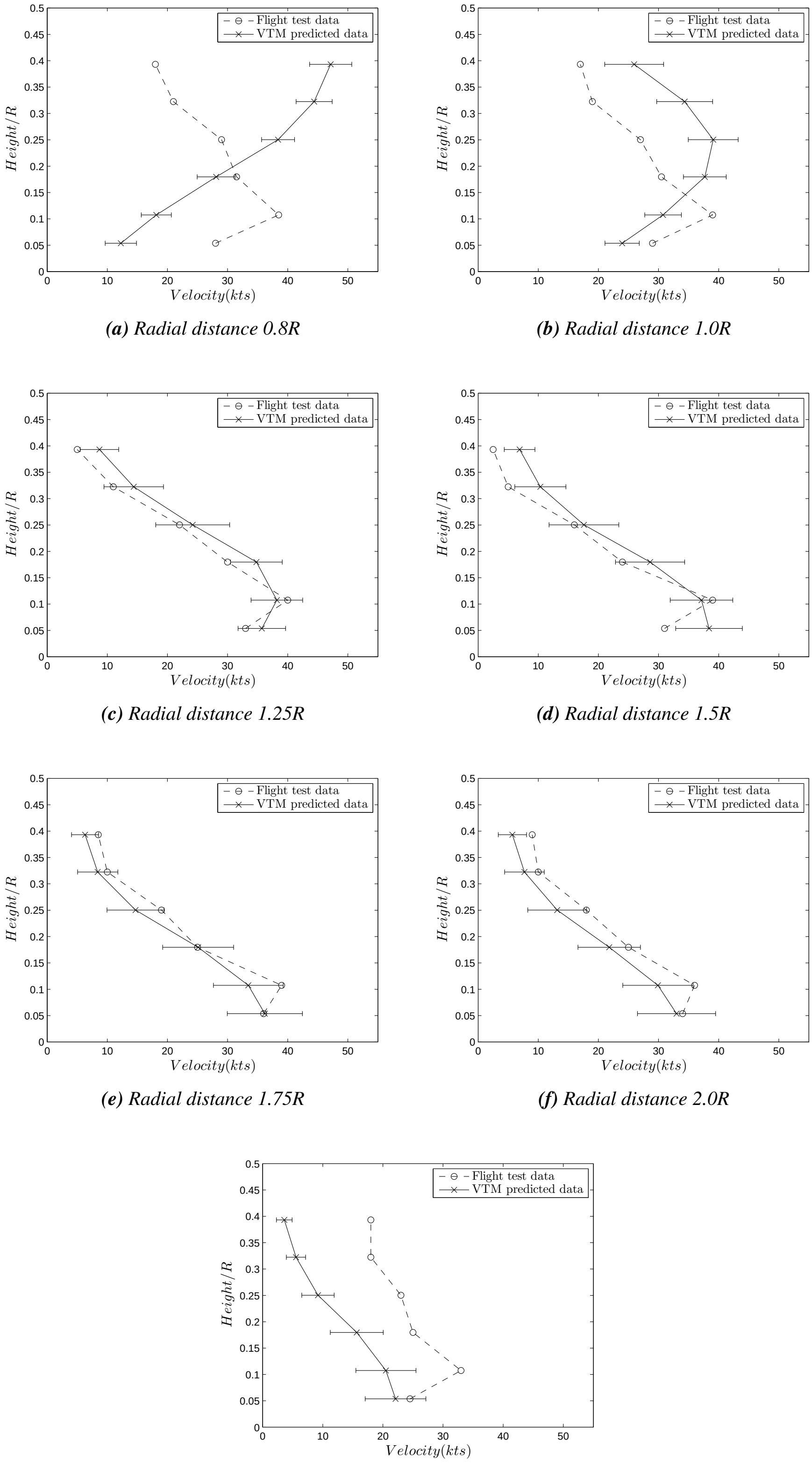

(a) Radial distance 0.8R

(b) Radial distance 1.0R

(c) Radial distance 1.25R

(d) Radial distance 1.5R

(e) Radial distance 1.75R

(f) Radial distance 2.0R

(g) Radial distance 3.0R

Figure 1: *Outwash velocity profiles below a CH-53E rotor hovering at a height of two rotor radii above the ground at a thrust coefficient of 0.007.*

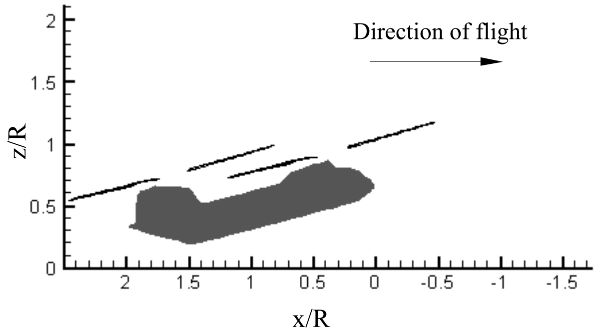

Figure 2: *Schematic of the tandem rotor configuration that was modelled using the VTM (fuselage represented solely for clarity, ground plane at $z/R = 0$).*

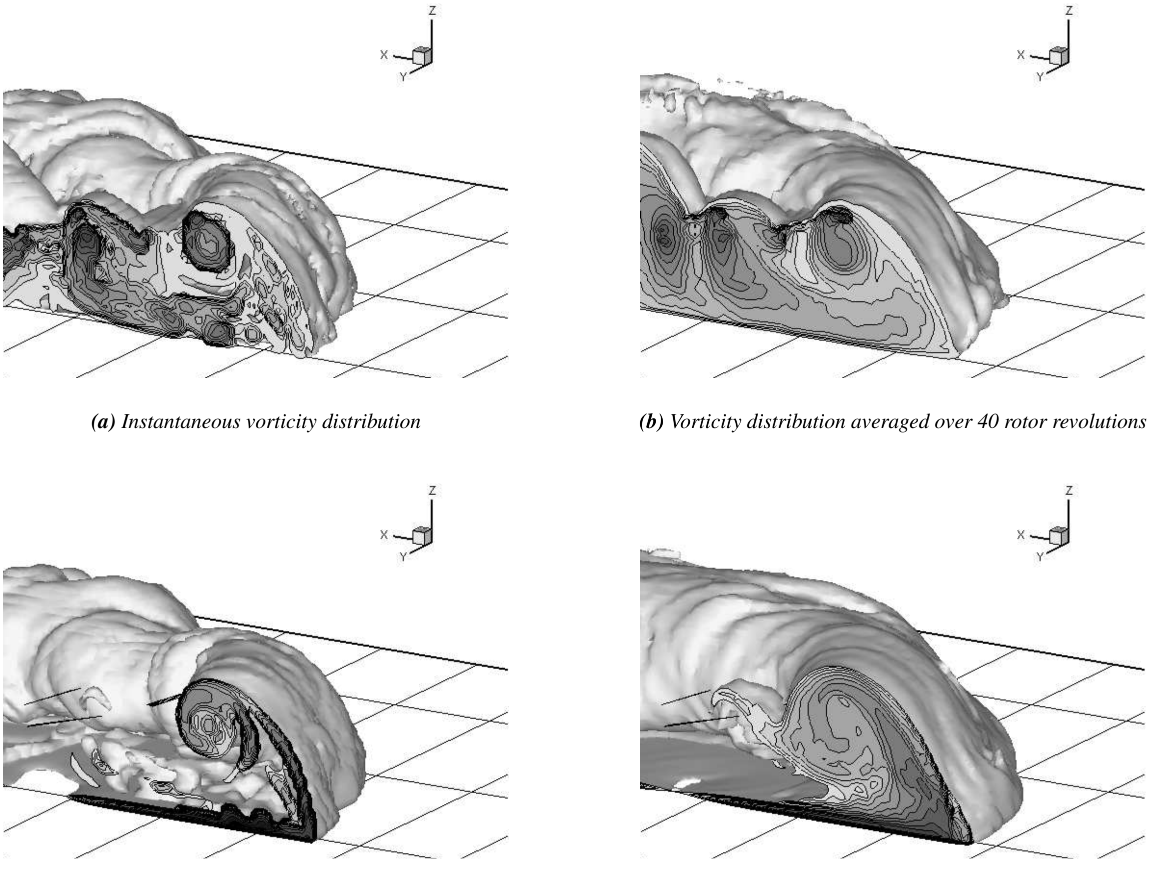

(a) *Instantaneous vorticity distribution*

(b) *Vorticity distribution averaged over 40 rotor revolutions*

(c) *Instantaneous dust density distribution*

(d) *Dust density distribution averaged over 40 rotor revolutions*

Figure 3: *Vorticity and dust distributions in the flow below a tandem rotor helicopter during a landing manoeuvre – normalised advance ratio $\mu^\star = 0.29$ ($\mu = 0.025$). Darker contours represent higher values of the variable within each plot.*

lished itself. Nevertheless, the comparison lends further support to previous evidence suggesting that the VTM is eminently capable of modelling the flow field around rotors in strong ground effect.

The Flow Field Produced By Tandem Rotors

The role of the flow field below the helicopter in establishing the dust cloud associated with brownout can be best understood be analysing the aerodynamics and resultant particle dynamics of isolated rotors in strong ground effect. To this end, the flow field that is formed around the rotors of a tandem helicopter has been analysed. The helicopter was modelled, as shown schematically in Fig. 2, as two isolated rotors set in a tandem configuration with a 12% overlap in area between the front and rear rotors. Each rotor was modelled to have a solidity of 0.085 and three blades with a linear twist of 8°. No

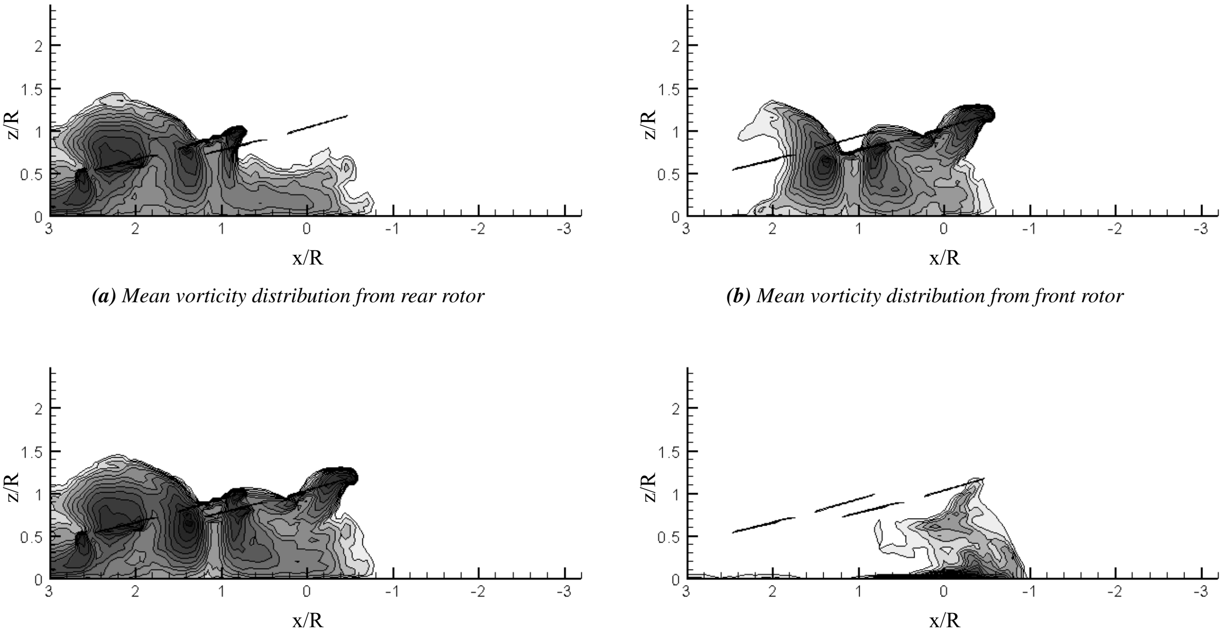

(a) Mean vorticity distribution from rear rotor

(b) Mean vorticity distribution from front rotor

(c) Combined vorticity distribution from both rotors

(d) Mean dust density distribution

Figure 4: *Vorticity and dust distributions in the flow below a tandem rotor helicopter during a landing manoeuvre – normalised advance ratio $\mu^\star = 0.47$ ($\mu = 0.04$). Darker contours represent higher values of the variable within each plot.*

fuselage was modelled so as to avoid complicating the interpretation of the flow field that is generated by the rotors of the helicopter. The simulated flight condition was set to be representative of a helicopter during a landing manoeuvre. In this vein, the rotors were modelled with a nose-up pitch attitude of 15° with the front rotor at a height of $0.88R$ above the ground, and the system was trimmed to an overall thrust coefficient of 0.0145 to represent a typical decelerating flight condition.

Figure 3 shows three-dimensional images of the vorticity and dust density distributions found in the flow field surrounding the rotors at a representative advance ratio $\mu^\star = 0.29$ ($\mu = 0.025$) during the simulated landing manoeuvre. The distributions have been sectioned through the longitudinal centreline of the helicopter to expose the internal details of the flow field. Parts (a) and (c) of the figure show the rather chaotic and disordered structure of the instantaneous dust and vorticity distributions in the flow whereas the mean distributions are better at revealing the persistent features of these distributions. For this reason, in the remainder of this paper, the dust and vorticity fields within the flow surrounding the helicopter will be presented almost exclusively after averaging over a significant number of rotor revolutions.

Figures 4, 5 and 6 show the vorticity distribution within the rotor wake at three different advance ratios during the simulated landing manoeuvre. In all these figures the vorticity magnitude on a vertical slice through the longitudinal centreline of the system has been plotted after averaging the vorticity distribution in the flow over approximately 40 revolutions.

Figure 4 shows the vorticity distribution in the flow around the rotors of the tandem helicopter when operating at a thrust normalised advance ratio $\mu^\star = 0.47$ ($\mu = 0.04$). Figure 4(a) shows the vorticity produced by the rear rotor and Fig. 4(b) shows separately the vorticity produced by the front rotor of the system. The combined vorticity field of both rotors is shown in Fig. 4(c). At this advance ratio and thrust coefficient, a single rotor with zero disc tilt would find itself within the recirculatory flow regime described by Curtiss *et al.* (Ref. 13). The calculations show however that the rearwards tilt of the rotors causes the rear rotor instead to form a prominent ground vortex which acts to entrain the vorticity from the leading edge of the front rotor and to prevent the vorticity field of the combined system from spreading very far ahead of the helicopter. The effect of the flow field on the distribution of dust that is entrained into the air from the ground below the helicopter is shown in Fig. 4(d), presented here as a contour map of dust density on a longitudinal slice through the centreline of the system. At this advance ratio, the dust cloud produced by the helicopter remains confined to a small zone of relatively stagnant flow forward of the ground vortex that is produced by the rear rotor. Most of the dust remains close to the ground, resulting in a relatively limited spatial region in which the cloud has significant density.

If the advance ratio is reduced somewhat, the flow changes character quite dramatically. Figure 5 shows the vorticity distribution near the rotors at $\mu^\star = 0.29$

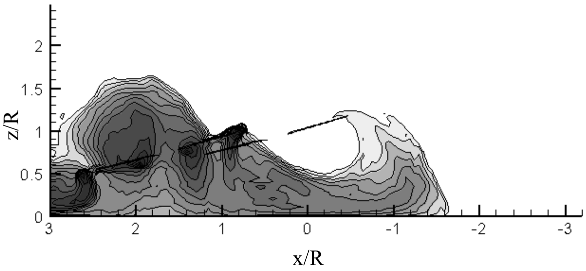

***(a)** Mean vorticity distribution from rear rotor*

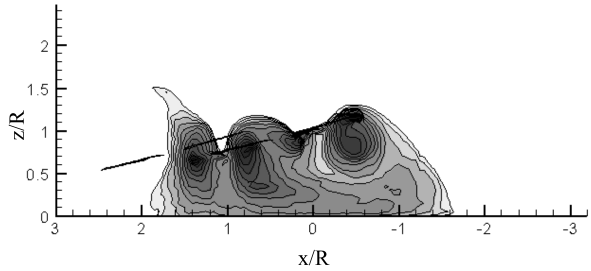

***(b)** Mean vorticity distribution from front rotor*

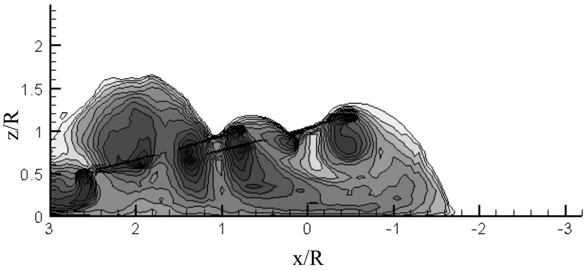

***(c)** Combined vorticity distribution from both rotors*

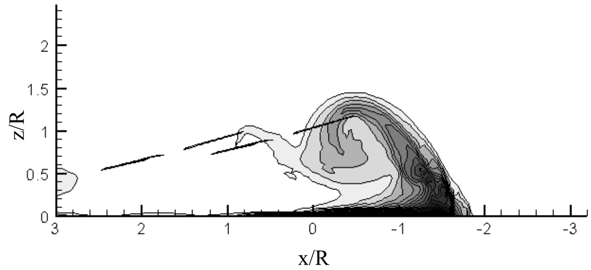

***(d)** Mean dust density distribution*

***Figure 5:** Vorticity and dust distributions in the flow below a tandem rotor helicopter during a landing manoeuvre – normalised advance ratio $\mu^{\star} = 0.29$ ($\mu = 0.025$). Darker contours represent higher values of the variable within each plot.*

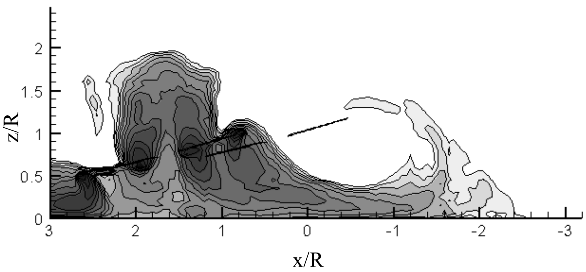

***(a)** Mean vorticity distribution from rear rotor*

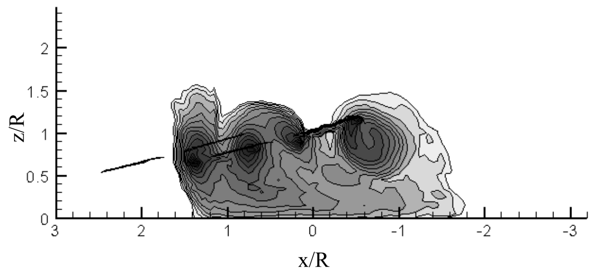

***(b)** Mean vorticity distribution from front rotor*

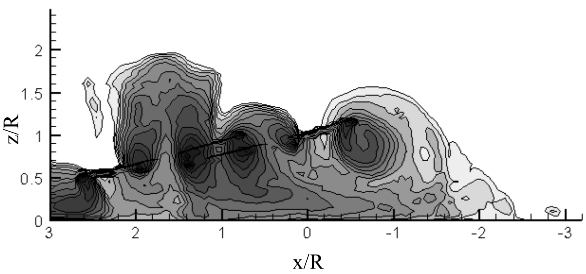

***(c)** Combined vorticity distribution from both rotors*

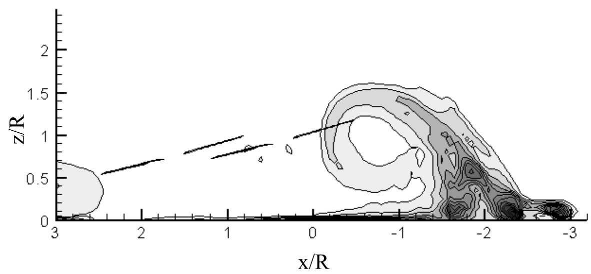

***(d)** Mean dust density distribution*

***Figure 6:** Vorticity and dust distributions in the flow below a tandem rotor helicopter during a landing manoeuvre – normalised advance ratio $\mu^{\star} = 0.12$ ($\mu = 0.01$). Darker contours represent higher values of the variable within each plot.*

($\mu = 0.025$). The predominant feature of the flow at this forward speed is the strong vortex that is produced by the roll-up of the wake of the front rotor immediately below its own leading edge. The flow produced by the front rotor is, in fact, strongly reminiscent of that found in the recirculatory regime of an isolated, single rotor. This vortex is strong enough to entrain a significant amount of vorticity from the rear rotor and to extend the combined vorticity distribution of the two rotors a significant distance out along the ground plane beyond the leading edge of the front rotor. This flow pattern results in significant entrainment of dust from the ground below the system. The subsequent recirculation of dust through the front rotor to form a dense wall of particulate matter just forward of the helicopter is clearly visible in Fig. 5(d).

This flow regime persists as the flight speed is reduced further. Figure 6 shows the flow near the rotors at a normalised advance ratio $\mu^\star = 0.12$ ($\mu = 0.01$). The overall structure of the wake is similar to that at $\mu^\star = 0.29$, but the vorticity field that is produced by the rear rotor extends somewhat further forward, even though it has a slightly reduced overall strength, than at the higher forward speed. Similarly, the vortex that is formed below the front rotor is somewhat larger, but is also weaker than at the higher forward speed. Nevertheless, as the wake extends further outwards below the rotors and interacts with a larger area of the ground plane, larger areas of dust are disturbed by the flow and subsequently contribute to the density of airborne particulate matter. The extent of the area of affected ground together with the existence of a strong recirculatory flow just above and behind the zone of maximum entrainment of dust from the ground results in the cloud of airborne dust that is created by the rotors being the largest at this forward speed, even though it has slightly lower overall density than at higher forward speeds. Figure 6(d) shows the dust cloud to consist again of a dense wall of dust approximately two rotor radii in front of the helicopter, but the recirculation of dust through the rotor also appears to be very effective in filling the void between this wall and the helicopter with a diffuse cloud of particulates. With the real aircraft it is surmised that this diffuse cloud of dust might pose a greater problem to the pilot in limiting his view of the ground directly in front of the cockpit than would the wall of dust some distance ahead of the aircraft.

The Link between Vorticity, Velocity and Dust Distribution

The clear link between the vorticity, or, equivalently, velocity distribution in the flow and the process of entrainment of dust from the ground plane into the airflow is revealed by comparing the time-averaged distribution of these parameters in the flow field of the tandem rotor system at advance ratio $\mu^\star = 0.47$ ($\mu = 0.04$) as shown in Fig. 7. Figure 7(a) shows the vorticity distribution around the rotors at this forward speed. Figure 7 (b) shows the associated time-averaged local speed of the flow, and Fig. 7(c) exposes the underlying topology of the flow by plotting a series of particle trajectories within the time-

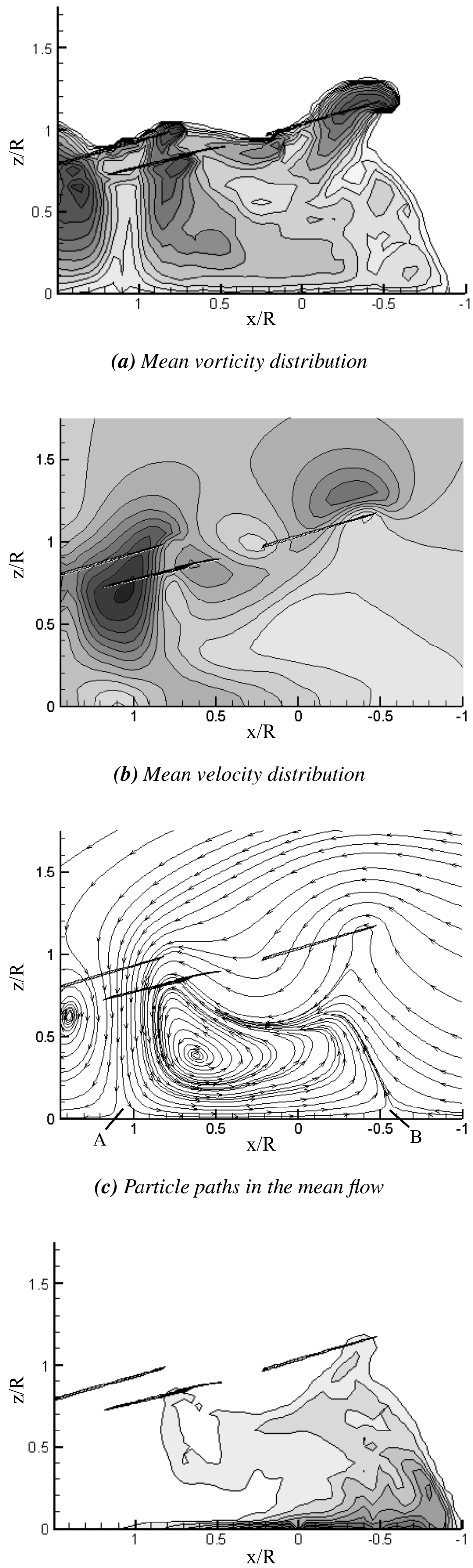

***(a)** Mean vorticity distribution*

***(b)** Mean velocity distribution*

***(c)** Particle paths in the mean flow*

***(d)** Mean dust density distribution*

***Figure 7:** Time-averaged vorticity, velocity and dust density in the flow below a tandem rotor during a landing manoeuvre – normalised advance ratio $\mu^\star = 0.47$ ($\mu = 0.04$). Darker contours represent higher values of the variable within each plot.*

averaged velocity field. Clearly apparent are the two stationary points in the flow field immediately adjacent to the ground plane, marked A and B in the figure. Bearing in mind the marked unsteadiness of the flow and hence the difficulty in relating the positions of these stationary points in the mean flow precisely to the positions of the stagnation points in the instantaneous velocity field, point A is located near to where the rotor downwash attaches to the ground plane, whereas point B is located near to the point at which the flow separates from the ground plane just upstream of the strong and very obvious ground vortex that is induced by the rear rotor at this advance ratio. The resultant time-averaged dust distribution in the flow around the rotors at this advance ratio is shown in Fig. 7(d).

At stationary point A (near $x/R = 1$), the velocity on the ground plane is effectively zero. The velocity on the ground plane increases steadily from point A towards the front of the rotor, however, and as the velocity exceeds the threshold for entrainment of particulates to occur, pick-up of dust from the ground plane initiates. The entrained material initially stays close to the ground plane, forming a thin, sheet-like layer that increases steadily in density through further entrainment of dust from the ground as it convects forwards towards the front of the helicopter. The sheet-like nature of the dust distribution is maintained by the downwards trajectory of the flow underneath the rotors. Forward of $x/R = 0$ though, the flow on the ground plane decelerates and the flow trajectory turns upwards until, at stationary point B, the speed of the flow is effectively zero and its trajectory vertically upwards. As a result, entrainment ceases and the dust layer on the ground thickens rather suddenly, forming the characteristic wedge-shaped 'separation zone' of high dust density that is visible between $x/R = 0$ and $x/R = -1$ in Fig. 7(d) as well as in almost all experimental visualisations of the brownout cloud (Ref. 19). Once the dust lifts off the ground and exits the separation zone, its dynamics are no longer controlled by the entrainment process but rather by the convective properties of the flow field. At the advance ratio represented in Fig. 7, the relatively weak velocity field just above the separation zone, together with the action of gravity in causing the particulate matter to fall out of the flow once entrained, leads to very little dust escaping from the separation zone and only a relatively diffuse and amorphous cloud of dust to be caught up in the flow behind the leading edge of the front rotor. At lower advance ratios (see Figs. 5 and 6), the initial formation of the dust sheet along the ground plane is very similar to that described here, but the strong recirculatory flow below the front rotor of the tandem helicopter is capable of drawing a significant amount of particulate material out of the separation zone and into the airflow in front of the rotor.

These observations suggest that a word of caution is in order to those who would propose that the vorticity distribution in the flow might be used as a 'surrogate' or 'tracer' for the dust distribution in the flow, thus obviating the need for the direct calculation of dust density distributions in addition to the fluid dynamics of the system if brownout is to be understood. Besides the obviously more intimate connection between the vorticity and velocity of the flow than between the particulate density and the velocity that is induced by the Biot-Savart relationship (leading to very different histories of the two distributions), the simple fact that the source of vorticity is on the rotor whereas the entrainment of dust into the flow occurs through a strongly non-linear and possibly even discontinuous process on the ground (as a result of the flow speed having to exceed the threshold velocity for entrainment to take place) leads to a very tenuous and superficial analogy between the vorticity and dust distributions that, at best, runs the risk of being too weak to be of practical use, and, at worst, is simply misleading.

The Effect of Blade Twist

There is a fair amount of anecdotal evidence that suggests that helicopters of different type are capable of generating dust clouds with rather different size and form. One of the key current problems is to determine which geometric features of the helicopter's configuration have greatest bearing on the size and shape of the dust cloud that is formed by the vehicle and, indeed, whether alteration of the geometric characteristics of the aircraft might have any effect on the geometry of the dust cloud that is produced by the helicopter during incipient brownout conditions. The VTM has been used to examine the effect of blade twist on the geometric characteristics of the brownout cloud that is produced by a tandem rotor helicopter. The same generic tandem configuration as described earlier but with two different rotor designs, one with 8° and the other with 12° of linear blade twist, was simulated during the same landing manoeuvre as described earlier. Figures 8 to 11 compare the flow and the resultant dust clouds produced by the rotors with the two different blade twist distributions at the same two advance ratios for which data was presented earlier in this paper. The data presented in the images have been averaged over approximately 25 revolutions after allowing the initial transients in the flow to dissipate.

The results of the limited comparison presented here are quite revealing. At the slower advance ratio, the overall size of the dust cloud is very similar for both rotor configurations. Particulate matter is recirculated through the front rotor to produce a dust cloud that extends above the height of the front rotor. The system with 8° of blade twist generates a concentration of dust that extends somewhat higher, and marginally further upstream along the ground plane, than does the dust cloud that is generated by the system with 12° of blade twist. The most prominent difference between the dust distributions that are generated by the two rotor configurations is that the concentration of dust within the flow field of the rotors with 8° of blade twist is significantly higher than when the rotors have 12° of blade twist. This difference can perhaps be explained by comparing the flows produced by the two systems along the ground plane in the entrainment zone between $x/R = 0.0$ and $x/R = -1.5$. It can

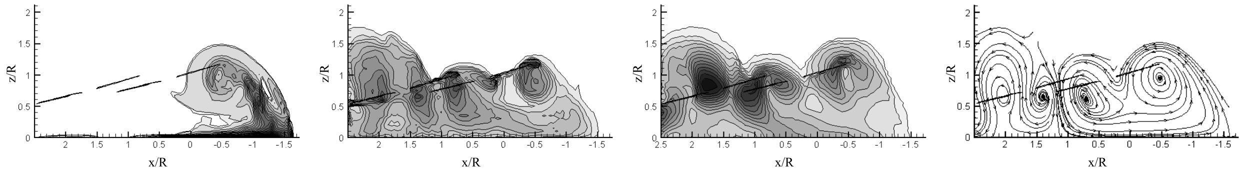

(a) Mean dust distribution *(b) Mean vorticity distribution* *(c) Mean velocity distribution* *(d) Particle paths in the mean flow*

Figure 8: *Distributions of vorticity, velocity and dust density below a tandem rotor with a blade twist of* 8° *during a landing manoeuvre – normalised advance ratio* $\mu^\star = 0.29$ *(*$\mu = 0.025$*). Darker contours represent higher values of the variable within each plot.*

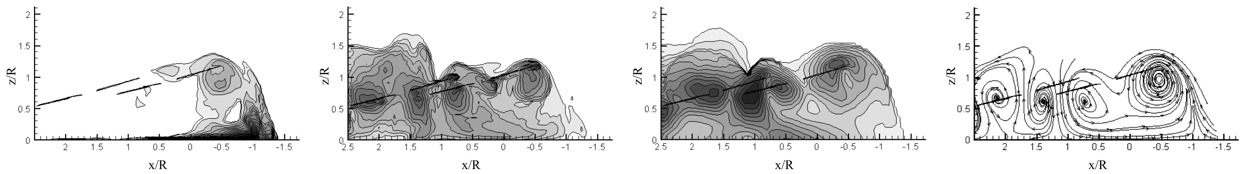

(a) Mean dust distribution *(b) Mean vorticity distribution* *(c) Mean velocity distribution* *(d) Particle paths in the mean flow*

Figure 9: *Distributions of vorticity, velocity and dust density below a tandem rotor with a blade twist of* 12° *during a landing manoeuvre – normalised advance ratio* $\mu^\star = 0.29$ *(*$\mu = 0.025$*). Darker contours represent higher values of the variable within each plot.*

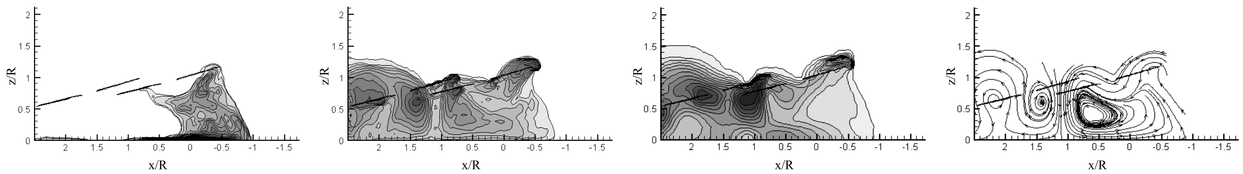

(a) Mean dust distribution *(b) Mean vorticity distribution* *(c) Mean velocity distribution* *(d) Particle paths in the mean flow*

Figure 10: *Distributions of vorticity, velocity and dust density below a tandem rotor with a blade twist of* 8° *during a landing manoeuvre – normalised advance ratio* $\mu^\star = 0.47$ *(*$\mu = 0.04$*). Darker contours represent higher values of the variable within each plot.*

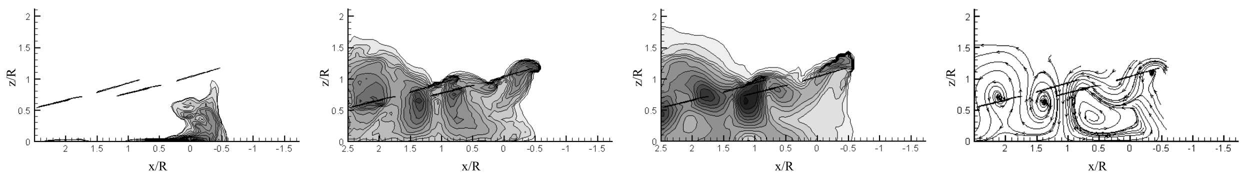

(a) Mean dust distribution *(b) Mean vorticity distribution* *(c) Mean velocity distribution* *(d) Particle paths in the mean flow*

Figure 11: *Distributions of vorticity, velocity and dust density below a tandem rotor with a blade twist of* 12° *during a landing manoeuvre – normalised advance ratio* $\mu^\star = 0.47$ *(*$\mu = 0.04$*). Darker contours represent higher values of the variable within each plot.*

be seen that the rotors with 12° of blade twist produce a somewhat lower level of mean vorticity within this region and that the velocities produced along the ground plane by this system are thus slightly lower than those produced by the rotors with 8° of blade twist. This would appear to cause less dust to be disturbed and entrained into the dust sheet below the rotors with the result that, as the ground jet decelerates, less dust is fed into the resultant separation zone subsequently to be drawn into the recirculation below the front rotor.

The effect of blade twist on the size of the dust cloud that is produced by the helicopter is more apparent at the higher advance ratio. Figures 10 and 11 show that both the height to which the dust cloud reaches and its forward extent along the ground plane is significantly greater when the rotors have a blade twist of 8° than when the blades have 12° of twist. This can be explained by noting that the calculations show the vorticity produced by the rotors with 8° of blade twist to travel further upstream against the oncoming flow than when the blades have 12° of twist. The associated region of high velocity along the ground plane thus also extends further upstream. It would appear that the larger region of contact of the wake with the ground plane results in an expanded entrainment zone and thus more dust to be disturbed and to end up in suspension when the rotors have low twist, resulting in the observed differences in the size of the dust clouds produced by the two systems at high advance ratio.

Conclusion

The Vorticity Transport Model, coupled to a new particle transport model, has been used to simulate the development of the dust cloud that forms when particulates are entrained into the flow surrounding a helicopter operating close to the ground in dusty or desert conditions. Under certain conditions the dust cloud can obscure the pilot's view of the ground, causing him to lose situational awareness in a potentially dangerous condition known as 'brownout'.

An important pre-requisite to modelling brownout accurately is to predict correctly the characteristics of the flow produced by helicopter rotors when operating in strong ground effect. Data is presented to show that the VTM is able to predict accurately the outwash velocities within the flow field below the rotor, lending further support to previous evidence which suggests the VTM is able to capture the important features of the flow field around a rotor in strong ground effect. Correct prediction of the outwash velocity is particularly important in the context of brownout modelling since the entrainment and transport of the particulates that eventually form the brownout cloud is closely related to the velocity distribution within the rotor wake.

The coupled VTM-particle transport model has been used to simulate the flow around a tandem rotor configuration during the final stages of landing. The time-averaged flow field around the helicopter is characterised by the existence of two stationary points immediately adjacent to the ground plane. The rearmost stationary point is associated with the attachment of the rotor-induced downwash to the ground. Almost all entrainment of dust into the flow takes place forward of this point; the dust initially remains in a thin, sheet-like layer above the ground. The second stationary point marks the most forward penetration of the wake against the oncoming flow. As the dust sheet approaches this point, the associated deceleration of the flow causes the layer to thicken and to form a characteristic wedge-shaped 'separation zone' just behind the forward stationary point. The amount of sand that is subsequently drawn up away from the ground to form the brownout cloud then appears to be critically dependent on the strength and position relative to the separation zone of strong regions of recirculation that are capable of drawing material out of this high-density reservoir of particulates and into the pilot's field of view.

VTM simulations suggest that, for a tandem rotor helicopter at least, the sudden growth of the dust cloud that is responsible for the onset of brownout as the forward speed of the helicopter is decreased may be due to a change in mode within the flow field surrounding the aircraft. At higher advance ratios the flow is dominated by a strong ground vortex that is created by the rear rotor. The forward extent of the resultant dust cloud is limited though by the absence of any strong recirculation within the flow below the front rotor of the system. At lower forward speed, however, the ground vortex of the rear rotor is replaced by a strong vortex that lies just below the leading edge of the front rotor. This vortex is responsible for drawing a significant amount of dust out of the surface layer of entrained particulates to form a dense wall of dust some distance upstream of the helicopter. The vortex also causes significant recirculation of dust through the front rotor where it may exacerbate the onset of brownout.

A study of the effect of blade twist on the strength and shape of the dust cloud that is formed in the flow surrounding helicopters with tandem rotors suggests that systems with smaller blade twist but the same disc loading might produce denser dust clouds than those with high blade twist. The significant factor governing the density of the dust cloud appears to be the strength of the ground jet just above the ground plane and hence the amount of particulate matter that is entrained into the separation zone subsequently to be convected into the flow surrounding the rotorcraft.

The results presented in this paper are highly suggestive but can hardly be considered as exhaustive or comprehensive in any way. Indeed, much further work needs to be done to investigate, and eventually to understand, the key parameters that govern the evolution of the dust cloud that is formed when a rotor wake interacts with the ground in dusty conditions. The numerical results presented here show significant structure to exist within the chaos of the swirling dust clouds as they envelop the cockpit of the helicopter during the onset of brownout, and, perhaps most importantly for future prospects of mitigating the onset of brownout through purely aerodynamic means, that the shape, size and density of the dust cloud is indeed sensitive to the aerodynamic configuration of the rotorcraft.

References

[1] Rogers, S.J., "Evaluation of The Dust Cloud Generated by Helicopter Rotor Downwash," USAAVLABS Technical Report 67-81, U.S. Army Aviation Material Laboratories, 1968.

[2] Cowherd, C., "Sandblaster 2 Support of See-Through Technologies for Particulate Brownout," MRI Project No. 110565.1.001, Midwest Research Institute, 2007.

[3] Keller, J.D., Whitehouse, G.R., Wachspress, D.A., Teske, M.E., and Quackenbush, T.R., "A Physics-Based Model of Rotorcraft Brownout for Flight Simulation Applications," 62nd Annual American Helicopter Society Forum, Phoenix, AZ, May 9-11 2006.

[4] Ryerson, C. C., Hachnel, R. B., Koenig, G. G., and Moulton, M. A., "Visibility Enhancement in Rotorwash Clouds," 43rd AIAA Aerospace Sciences Meeting and Exhibit, Reno, Nevada, 10-13 Jan. 2005.

[5] Haehnel, R.B., Moulton, M.A., Wenren, Y., and Steinhoff, J., "A Model to Simulate Rotorcraft-Induced Brownout," 64th Annual Forum of the American Helicopter Society, Montréal, 2008.

[6] Brown, R. E., "Rotor Wake Modeling for Flight Dynamic Simulation of Helicopters," *AIAA Journal*, Vol. 38 (1), January 2000, pp. 57–63.

[7] Brown, R. E. and Line, A. J., "Efficient High-Resolution Wake Modelling Using the Vorticity Transport Equation," *AIAA Journal*, Vol. 43 (7), July 2005, pp. 1434–1443.

[8] Phillips, C. and Brown, R.E., "Eulerian Simulation of the Fluid Dynamics of Helicopter Brownout," 64th Annual Forum of the American Helicopter Society, Montréal, 2008.

[9] White, B.R., "Soil Transport by Winds on Mars," *Journal of Geophysical Research*, Vol. 84 (B9), August 1979, pp. 4643–4651.

[10] Lu, H. and Shao, Y., "Toward Quantitative Prediction of Dust Storms: An Integrated Wind Erosion Modelling System and its Applications," *Environmental Modelling and Software*, Vol. 16 (3), April 2001, pp. 233–249.

[11] Marticorena, B. and Bergametti, G., "Modeling the Atmospheric Dust Cycle: 1. Design of a soil-derived dust emission scheme," *Journal of Geophysical Research*, Vol. 100 (D8), August 1995, pp. 16415–16430.

[12] Brown, R. E. and Whitehouse, G. R., "Modelling Rotor Wakes in Ground Effect," *Journal of the American Helicopter Society*, Vol. 49 (3), July 2004, pp. 238–249.

[13] Curtiss, H. C. Jr., Erdman, W., and Sun, M., "Ground Effect Aerodynamics," *Vertica*, Vol. 11 (1-2), 1987, pp. 29–42.

[14] Hayden, J. S., "The Effect of the Ground on Helicopter Hovering Power Required," 32nd Annual Forum of the American Helicopter Society, Washington, D.C., 10-12 May 1976.

[15] Knight, M. and Hefner, R.A., "Static Thrust Analysis of the Lifting Airscrew," T.N. No. 626, 1937.

[16] Cooke, A.K. and Fitzpatrick, E.W.H., *Helicopter Test and Evaluation*, American Institute of Aeronautics and Astronautics Education Series, Reston, VA, 2002.

[17] Harris and Simpson, "CH-53E Helicopter Downwash Evaluation," NATC SY-89R-78, August 1978.

[18] Preston, J.R., "VTOL Downwash / Outwash Operational Effects Model," American Helicopter Society 50th Annual Forum, Washington DC, May 1994.

[19] Nathan, N.D. and Green, R.B., "Measurements of a Rotor Flow in Ground Effect and Visualisation of the Brown-out Phenomenon," 64th Annual Forum of the American Helicopter Society, Montréal, 2008.